ELSEVIER

Neurobiology of Aging 31 (2010) 280–289

NEUROBIOLOGY OF AGING

www.elsevier.com/locate/neuaging

The heat shock response modulates transthyretin deposition in the peripheral and autonomic nervous systems

Sofia Duque Santos [a], Rui Fernandes [b], Maria João Saraiva [a,c,*]

[a] *Molecular Neurobiology Unit, Institute for Molecular and Cell Biology – IBMC, 4150-180 Porto, Portugal*
[b] *Advanced Tissue Analysis Facility, Institute for Molecular and Cell Biology – IBMC, 4150-180 Porto, Portugal*
[c] *Instituto de Ciências Biomédicas de Abel Salazar, University of Porto – ICBAS, 4099-003 Porto, Portugal*

Received 4 October 2007; received in revised form 27 March 2008; accepted 1 April 2008
Available online 15 May 2008

Abstract

Familial amyloidotic polyneuropathy (FAP) is a neurodegenerative disease that selectively affects the peripheral nervous system. The putative cause of this life threatening pathology is tissue deposition of mutant transthyretin (TTR), initially as non-fibrillar deposits and later as fibrillar material. The mouse models currently available do not recapitulate the human whole features, since the peripheral nervous tissue is spared. We have characterized a new mouse model expressing the human transthyretin V30M in a heat shock transcription factor 1 (Hsf1) null background. The lack of HSF1 expression leads to an extensive and earlier non-fibrillar TTR, evolving into fibrillar material in distinct organs including the peripheral nervous system. Furthermore, inflammatory stress and a reduction in unmyelinated nerve fibers were observed, as in human patients. These results indicate that HSF1 regulated genes are involved in FAP, modulating TTR tissue deposition. The novel mouse model is of the utmost importance in testing new therapeutic strategies and in addressing the influence of the stress response in misfolding diseases.

Keywords: Transthyretin; Amyloid; Peripheral nervous system; Familial amyloidotic polyneuropathy; Neurodegeneration; Heat shock transcription factor; Heat shock protein

1. Introduction

Several hereditary mutations in human plasma transthyretin (TTR) have been identified and related to familial amyloidotic polyneuropathy (FAP). The most common TTR variant is the substitution of a valine for a methionine at position 30 – TTR V30M (Saraiva et al., 1984) resulting in a destabilized protein that easily aggregates, deposits in tissues and forms fibrils. It is a systemic pathology with the peripheral nervous system (PNS) selectively affected (Coimbra and Andrade, 1971 and reviewed by Sousa and Saraiva, 2003). FAP patients can be classified according to degree and type of deposition present in nerves and fiber degeneration and scored from FAP 0–3 (Sousa et al., 2001a): (i) FAP 0 – no fiber degeneration, no amyloid but non-fibrillar TTR deposition; (ii) FAP 1 – mild degeneration, discrete TTR fibrils; (iii) FAP 2 – considerable degeneration, abundant amyloid; (iv) FAP 3 – severe degeneration and extensive amyloid deposits. The unmyelinated fibers are first affected while the myelinated fibers degenerate later.

A suitable transgenic mouse model for the study of FAP pathology and treatment is crucial. Several groups have generated transgenic mice carrying the human *ttr* V30M gene (Nagata et al., 1995; Sasaki et al., 1986; Yamamura et al., 1987) However, TTR deposition in the peripheral and autonomic nervous systems was to date, never observed. In our laboratory, transgenic mice expressing the human TTR L55P, one of the most aggressive human variant TTR found in nature, were generated (Sousa et al., 2002). When compared to the TTR V30M mice, the TTR L55P mice present earlier, non-fibrillar TTR deposition starting at 1–3 months. At 4–8 months fibrillar deposits in the GI tract and skin are detected.

* Corresponding author at: Molecular Neurobiology Unit, Institute for Molecular and Cell Biology, Rua do Campo Alegre 823, 4150-180 Porto, Portugal. Tel.: +351 226074900; fax: +351 226099157.
E-mail address: mjsaraiv@ibmc.up.pt (M.J. Saraiva).

0197-4580/$ – see front matter © 2008 Elsevier Inc. All rights reserved.
doi:10.1016/j.neurobiolaging.2008.04.001

In contrast with these results, TTR L55P transgenic mice performed in another laboratory did not show TTR deposits, even in old animals, which was probably related to the low number of transgene copies (one or two) (Teng et al., 2001). In any case, non-fibrillar or fibrillar deposits were never detected in the peripheral and autonomic nervous systems, even at old ages.

Activation of NF-κB has been observed in FAP nerves (Sousa et al., 2000) and salivary glands (Sousa et al., 2005) involving activation of the receptor for advanced glycation end products (RAGE) – (Sousa et al., 2001b) triggering inflammatory and oxidative pathways. Thus, TTR deposits into tissues lead to cellular stress and increased pro-inflammatory molecules, such as tumor necrosis factor-alpha (TNF-α), interleukin1-beta (IL1-β) – (Sousa et al., 2001b) and activated caspase-3. One possible defence mechanism in harsh extracellular conditions is the stress response; therefore, disruption of this pathway could be affected or affect TTR amyloidosis.

To test this hypothesis we crossed mice lacking the main heat shock transcription factor (Hsf1) (Xiao et al., 1999), with transgenic mice expressing the human TTR V30M.

This model represents a closer approach to the study of FAP and opens new possibilities for the involvement of the stress response in this neurodegenerative disease.

2. Material and methods

2.1. Animals

Hsf1-KO mice (Hsf1tm1Ijb) in the BALB/c × 129 SvEv hybrid background were a kind gift from Dr Ivor Benjamin from Utah Health Sciences Center, USA (Xiao et al., 1999). The mice were backcrossed to congenic 129/Sv mice as described previously (Santos and Saraiva, 2004). By crossing homozygous males with heterozygous females (since homozygous females are infertile) we have obtained 22% homozygous mice for Hsf1 (from a total of 229 pups). By mating Hsf1-KO mice with transgenic mice for human TTR V30M carrying the human homologous promoter (Nagata et al., 1995) Tg(6.0-hV30M)14Imeg (labelled **TTR mice**) for more than 9 generations we obtained TTRV30M/Hsf1-KO (labelled **TTR/HSF1 mice**). A similar survival rate of homozygous mice for Hsf1 was obtained (24%). Both the original and final strains were all in the 129/Sv background.

The animals were housed in pathogen-free conditions, in a controlled temperature room, maintained under a 12 h light/dark period. Water and food were freely available. All animal experiments were carried out in accordance with the European Communities Council Directive.

2.2. Tissue analysis

Mice were anesthetised with 1 mg/kg medetomidine, 75 mg/kg ketamine administered intraperitoneally, sacrificed, and the organs of interest were collected, fixed in neutral buffered formalin and embedded in paraffin. The same tissues were collected and frozen immediately in dry ice and stored at −70 °C until use. Congo red staining was performed as described by Puchtler and Sweat (1965). For immunohistochemistry, primary antibodies included: rabbit anti-human TTR (1:1000, DAKO, Denmark); goat anti-TNF-α (1:25, Santa Cruz Biotechnology, Inc., USA); goat anti-IL1-β (1:25, Santa Cruz Biotechnology, Inc., USA); mouse anti-MCP-1 (1:1000, Chemicon, USA); mouse monoclonal NCL-MACRO (1:100, NOVOcastra, UK); rabbit anti-RAGE (1:50, Santa Cruz Biotechnology, Inc., USA); rabbit anti-NF-κB (1:500, Santa Cruz Biotechnology, Inc., USA); goat anti-Hsp70 (1:25, Santa Cruz Biotechnology, Inc., USA). Corresponding secondary antibodies used were: biotin-conjugated (1:20 Sigma, USA), followed by extravidin labelling (1:20, Sigma, USA). Mouse monoclonal antibodies were used with the MOM kit (Vector) according to the supplier's instructions. The reaction was developed with 3-amino-9-ethyl carbaxole, AEC (Sigma, USA) or 3,3′-diaminobenzidine DAB (Sigma, USA). In some control experiments, the primary antibody was replaced by blocking buffer; control analysis of TTR staining included pre-absorption with human recombinant TTR as described before (Sousa et al., 2002).

Semi-quantitative analysis of immunohistochemical slides was performed using Scion image quant program that measures the area occupied by the substrate reaction colour and normalized to the total image area. Mean values of % occupied area are displayed with the corresponding standard deviation. Each animal tissue was evaluated in four different areas. Statistical analyses were performed by a two-tailed, paired Student's *t*-test. The significance level was set at $*p < 0.02$ and $**p < 0.002$.

Presence of human TTR in parasympathetic ganglia of the stomach and intestine was studied by double immunofluorescent staining with rabbit anti-human TTR (1:1000, DAKO, Denmark) and mouse anti-PGP9.5 (1:40, Serotec, USA) as the primary antibodies; secondary antibodies were, respectively: anti-rabbit Alexa Fluor 488 (Molecular probes, UK) and goat anti-mouse Alexa Fluor 568 (Molecular probes, UK). Slides were mounted with vectashield (Vector) and visualized in a Zeiss Cell Observer System microscope (Carl Zeiss, Germany) equipped with filters for FITC and rhodamine like dyes.

Hsp70 expression was investigated in mice tissues extracts by Western blotting. Total homogenates were centrifuged at 16,000 × *g* for 30 min and supernatants analyzed by Hsp70 immunoblot (1:100, Santa Cruz Biotechnology, Inc., USA). The same amount of protein was loaded as visualized by β-actin immunoblot (1:5000, Sigma, USA).

2.3. Tissue TTR extraction

TTR deposits were extracted in selected tissues by the method of Kaplan et al. (1994). The extracts were loaded on

a 15% SDS polyacrylamide gel. The Western blot was probed for human TTR (anti-TTR, 1:1,500, DAKO, Denmark) and developed with Super Signal West Pico (Pierce, USA).

2.4. Electron microscopy

Sciatic nerves from 24 months old TTR/HSF1 mice, positive for TTR deposition as assessed by immunohistochemistry, were fixed in 1% glutaraldehyde o/n at 4 °C and washed in PBS. Tissues were embedded in Epon resin and ultrathin sections (500 Å) were cut onto copper grids. Grids were stained first with uranyl acetate and then lead citrate followed by observation in a Zeiss 10C electron microscope. For immunoelectron microscopy sciatic nerves were embedded in LR white resin and ultrathin sections (500 Å) were cut onto nickel grids. Grids were incubated with sheep anti-human TTR antibody (1:100, The Binding Site) o/n at 4 °C. Control grids were incubated without TTR antibody.

2.5. Morphometric studies

Sciatic nerves from: 12 months old TTR/HSF1 mice with ($n = 6$) and without ($n = 6$) TTR deposition (as assessed by immunohistochemistry), 24 months TTR/HSF1 mice with TTR deposition ($n = 6$), and 12 and 24 months TTR control mice ($n = 6$, each), were collected, fixed in 1% glutaraldehyde in PBS overnight at 4 °C and washed in sodium cacodylate (0.1 M, pH 7.4). The nerves were fixed in osmium tetroxide before dehydration and embedding in Epon resin. Semithin sections (1 μm) were cut from Epon-embedded blocks and stained in toluidine blue for myelinated fiber counting. This counting was performed in the whole nerve area using 20× amplified photomicrographs. Ultrathin transverse sections (500 Å) were cut onto copper grids, stained with uranyl acetate and lead citrate and visualized in a Zeiss 10C electron microscope for unmyelinated fiber counting. For each animal, 10 photomicrographs amplified 10,000× were taken, corresponding to approximately 3000 mm^2.

3. Results

3.1. TTR deposition in extra-neural tissues

We studied TTR deposition in extra-neural tissues in TTR/HSF1 mice at different ages. The GI tract presented TTR deposition as non-fibrillar aggregates at all ages analyzed (1 month until 24 months, with an average of 12 animals for each age group, respectively, 3,6,12 and 24 months) (not shown). By comparison to the previous mouse TTR model in the wild type background (Sousa et al., 2002), a two- to three-fold higher penetrance of TTR deposition was observed. For instance, at the age of 12 months, TTR deposition in the stomach is observed in 100% of TTR/HSF1 mice without endogenous TTR, while for TTR mice in the wild type background without endogenous TTR, only 52% of animals showed TTR deposits. Thus, TTR/HSF1 mice show an increased and more extensive TTR deposition in the GI tract, particularly in the stomach, related to Hsf1 disruption. This higher penetrance was also evident in TTR/HSF1 transgenic mice heterozygous for Hsf1, indicating that HSF1 modulates and increases TTR tissue deposition.

The skin was also evaluated as a site of major deposition and the penetrance of deposition in TTR/HSF1 mice was again different in comparison to the previous transgenic TTR mice characterized in our laboratory (Sousa et al., 2002). TTR/HSF1 mice showed TTR deposition in the skin as early as 3 months. The penetrance of TTR deposition ranged from 60% to 83% depending on the age (from 3 to 24 months) while in the previous transgenic model no deposition was obtained at the age of 3 months.

Amyloid was evaluated by Congo red staining (not shown) and was detected in the stomach as early as 6 months of age. For older ages, amyloid deposition was not extended to other organs, but a higher number of animals presented amyloid in the stomach.

3.2. TTR deposition in the nervous system

While analyzing the central (CNS), peripheral (PNS) and autonomic nervous systems of TTR/HSF1 mice we observed, for the first time, TTR deposition in the sciatic nerve, dorsal root ganglia (DRG), and autonomic ganglia (Fig. 1A), similarly to what is observed in FAP human patients. TTR deposition in DRG from 3-month old TTR/HSF1 mice affected from 33 to 73% of animals ($n = 16$). From 6 months onwards the percentage of DRG with TTR deposition increased and varied between 55 and 100% ($n = 48$). The percentage of TTR/HSF1 mice with deposition in the sciatic nerve compared to DRG was approximately 1/3 at 3 months, 1/2 at older ages (6, 12 months) and similar at 24 months (86% for sciatic nerve and 100% for DRG).

In DRG neurons, TTR was observed around the cell bodies in close contact with satellite cells (Fig. 1A). TTR was deposited extracellularly in the connective tissue between myelinated or unmyelinated fibers of the sciatic nerve and close to Schwann cells (Fig. 1A).

The right panels of Fig. 1A represent photomicrographs of CNS tissues that lack TTR deposition: brain and spinal cord. This distribution is in accordance with the human situation, as the CNS is spared in the vast majority of V30M patients.

We also investigated the TTR/HSF1 autonomic nervous system, particularly the parasympathetic system. Part of parasympathetic ganglia in smooth muscle layers of stomach and intestine presented TTR deposition, surrounding neurons, as investigated by double labeling with the neuronal marker PGP9.5 (Fig. 1A, bottom right panel).

Amyloid was not detected in the nervous system by Congo red, even at the age of 24 months; however, upon inspection with higher detail by electron microscopy, fibrillar material was visualized in sciatic nerve (Fig. 1B, arrow in the left

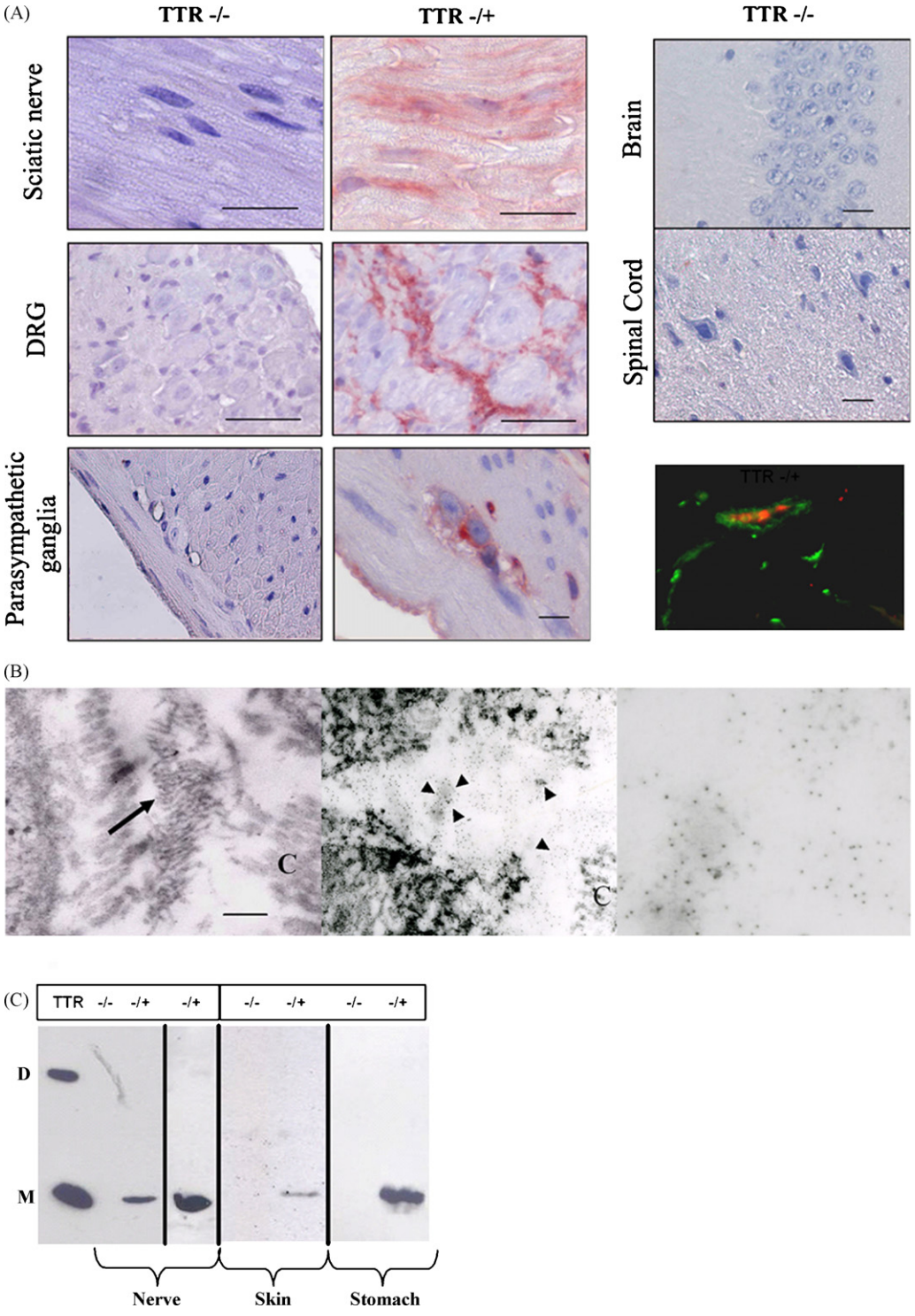

Fig. 1. TTR deposition in CNS, PNS and autonomic nervous systems of TTR/HSF1 mice. (A) *Left 2 columns*: optic microscopy demonstrating the absence (−/−) and presence (−/+) of TTR deposits in the sciatic nerve, DRG and parasympathetic ganglia of stomach in TTR/HSF1 mice. *Right upper column*: absence of TTR deposits in CNS, namely in the brain (hippocampus) and spinal cord. Scale bars 20 μm. *Right lower picture*: parasympathetic ganglia of a TTR positive intestine labelled by double immunofluorescence (merged image) for TTR (green) and PGP9.5 (red). (B) *Left picture*: electron microscopy image of the sciatic nerve from a 24-month TTR/HSF1 animal, positive for TTR deposition. Arrows indicate fibrillar material; C–collagen. Scale bar: 200 nm. *Middle picture*: immunoelectron microscopy of a TTR positive sciatic nerve, recognizing TTR deposits (arrowheads). *Right picture*: ampliation of the middle picture area, with TTR aggregates. (C) Protein aggregates extracted from nerve, skin and stomach of TTR/HSF1 mice, classified by immunohistochemistry as negative (−/−) or positive (−/+) for human TTR, analyzed by Western blotting using anti-human TTR. *Left lane*: standard human recombinant TTR; M: TTR monomer; D: TTR dimer.

panel) in the same fashion as in human clinical samples, i.e., it occurs extracellularly next to the basal membrane of Schwann cells and contiguous to collagen fibrils, replacing endoneurial contents (Sousa and Saraiva, 2003). Immunoelectron microscopy identified TTR as the component of the fibrillar material that is observed close to nerve fibers, in proximity to collagen (Fig. 1B, in the middle (arrowheads) and right panels).

These aggregated protein deposits were extracted from nerve, skin and stomach of selected positive or negative tissues for TTR deposition (as assessed previously by immunohistochemistry) and blotted for human TTR; the results (Fig. 1C) confirmed once again the immunohistochemical data, i.e., protein deposits in tissues were composed of TTR.

3.3. Inflammatory pathways

The pro-inflammatory cytokines, TNF-α and IL1-β, known to increase in human FAP nerves were evaluated by semi-quantitative immunohistochemistry in 6-month old TTR/HSF1 sciatic nerves with and without TTR deposition (Fig. 2). TNF-α levels (Fig. 2A) were markedly increased in mice having deposited TTR in the sciatic nerve ($p < 0.02$) in comparison to nerves without deposition. The levels obtained for the control groups (Hsf1-KO and wt mice) were similar to TTR/HSF1 sciatic nerves without deposition, meaning that the observed increase for TNF-α is related exclusively to TTR deposition in peripheral nerve. The same situation was evident in DRG, i.e., an increase in TNF-α levels occurred in neurons from ganglia presenting TTR deposition (Fig. 2A). Furthermore, transgenic TTR mice with the wild type Hsf1 allele presented TNF-α staining as wt mice (not shown), which is expected since TTR deposition is not found in these tissues.

Concerning IL1-β, an increase in expression was clearly observed in sciatic nerve and DRG from animals with TTR deposition versus without deposition (Fig. 2B); nerve from wild type animals did not label with anti-IL1-β whereas in Hsf1-KO nerve a slight staining was detected, probably

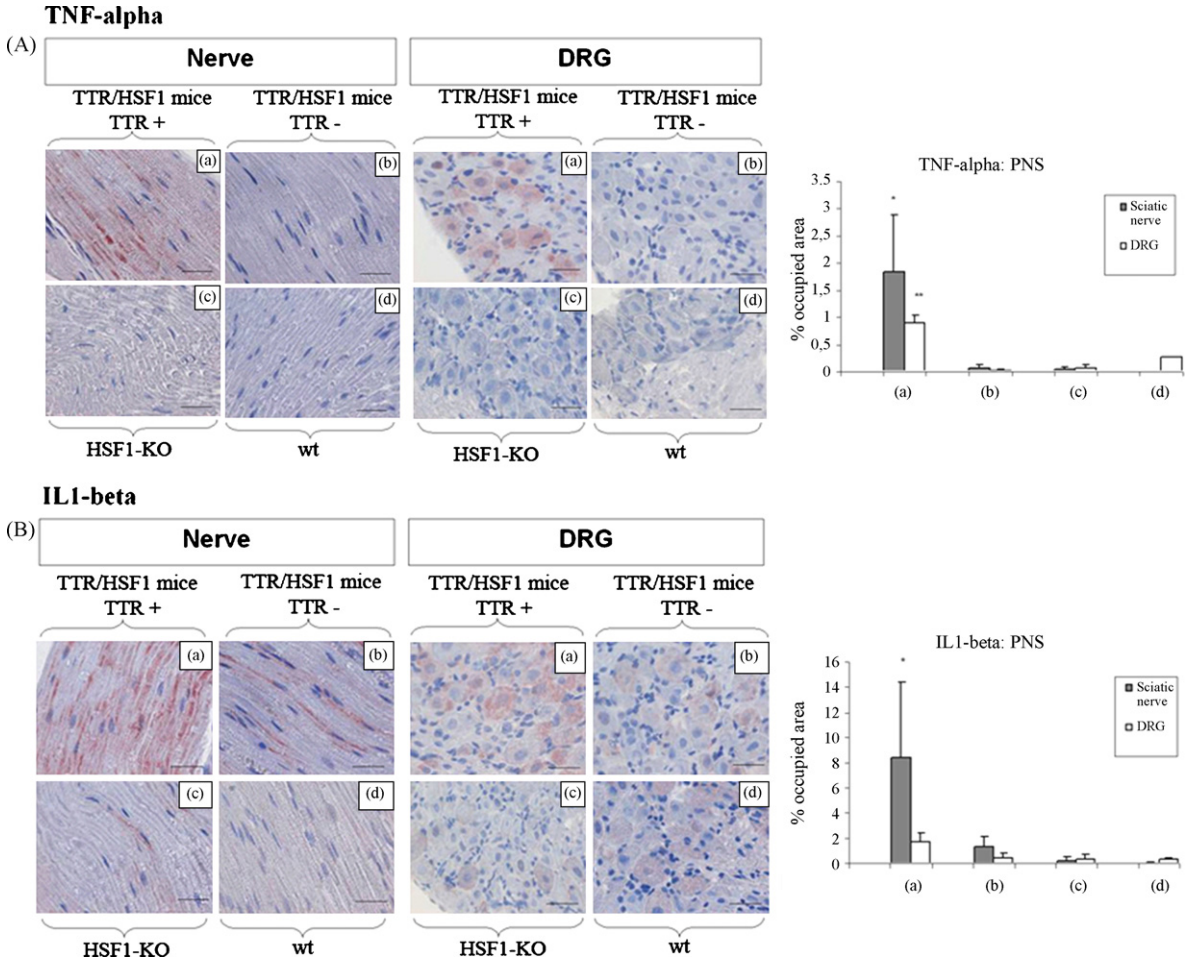

Fig. 2. Pro-inflammatory cytokines in the PNS of TTR/HSF1 mice. TNF-α (A) and IL1-β (B) in sciatic nerve and DRG of: (a) TTR/HSF1 positive (−/+) for human TTR ($n = 5$); (b) TTR/HSF1 negative (−/−) for human TTR ($n = 5$); (c) Hsf1-KO mice ($n = 7$); (d) wild type mice ($n = 6$); Scale bar 30 μm. *Charts*: semi-quantitative analysis of TNF-α and IL1-β in the sciatic nerve and DRG, using Scion image quant program, showing a significant increase in their expression in tissues with TTR deposition. $^{*}p < 0.02$, $^{**}p < 0.002$.

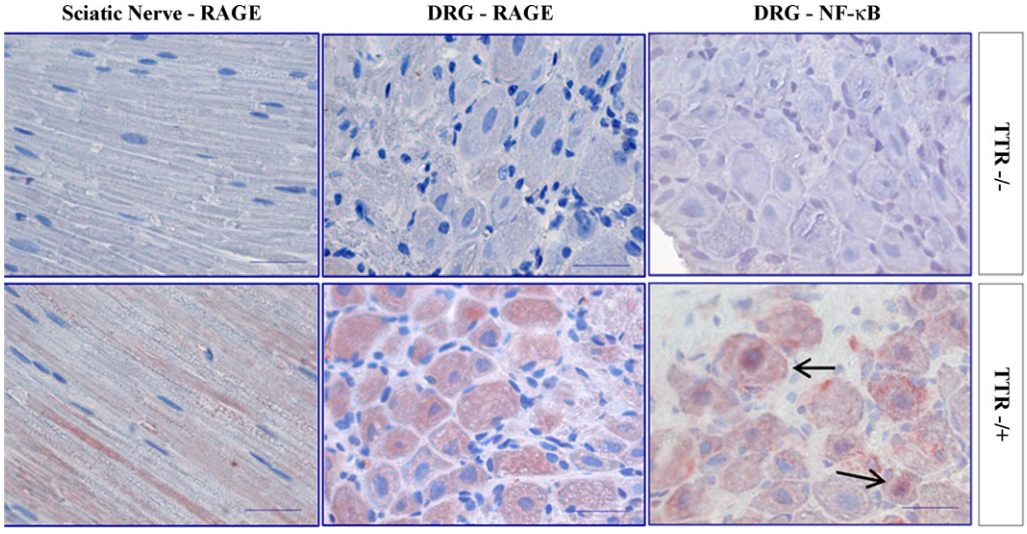

Fig. 3. RAGE expression and NF-κB activation in the PNS of TTR/HSF1 mice. *Left and middle panels*: RAGE immunostaining in sciatic nerve and DRG of TTR/HSF1 mice without (−/−; $n=8$) and with (−/+; $n=8$) TTR deposition. *Right panels*: expression of NF-κB in TTR/HSF1 DRG. Arrows indicate translocation to the nucleus. Scale bar 30 μm.

related to Hsf1 disruption. Transgenic TTR mice showed IL1-β staining similar to wt mice in these tissues (not shown).

Taken together, expressions of these cytokines (TNF-α and IL1-β) are indicative of ongoing inflammatory pathways related to TTR deposition in the PNS in a similar fashion as in FAP.

The expression of other proteins related to inflammation, previously tested in FAP tissues, were evaluated in TTR/HSF1 sciatic nerve and DRG, namely, RAGE, NF-κB, MCP-1 and NCL-MACRO (macrophage marker). In humans it is known that deposition of TTR V30M in nerve triggers NF-κB activation (Sousa et al., 2000) and that RAGE is involved in this pathway (Sousa et al., 2001b). TTR/HSF1 nerves and DRG without TTR deposition did not show, as expected, increased expression of RAGE and/or NF-κB translocation to the nucleus, while on average half of the TTR positive nerves and DRG displayed an increase in RAGE expression, and NF-κB translocation to the nucleus (Fig. 3) as seen in FAP patients. Levels of MCP-1, NCL-MACRO were not up-regulated in TTR/HSF1 sciatic nerve or DRG with or without the presence of TTR (data not shown) as in humans clinical samples.

3.4. Morphometry

We evaluated the number of unmyelinated (UMF) and myelinated (MF) fibers in the sciatic nerves of TTR/HSF1 mice versus age matched control TTR transgenic mice without TTR deposition, aged 12 and 24 months, respectively (Fig. 4, chart). The average densities in 12 months TTR/HSF1 mice with and without TTR deposition were similar: the UMF density was 107324 ± 35580 fibers/mm^2 for sciatic nerves without TTR deposition and 84506 ± 19643 fibers/mm^2 for sciatic nerves with TTR deposition; MF density in animals without TTR deposition was 17712 ± 2045 fibers/mm^2 while for nerves

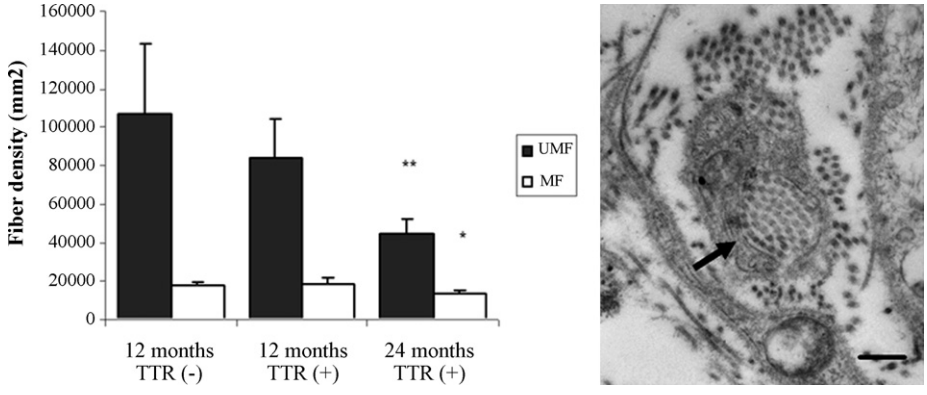

Fig. 4. Morphometric analysis of TTR/HSF1 nerve fibers. *Left chart*: Comparative unmyelinated and myelinated fiber densities in TTR positive ($n=6$) and negative ($n=6$) 12 months and in TTR positive 24 months ($n=6$) TTR/HSF1 sciatic nerves, documented in the right pictures. *$p<0.02$, **$p<0.002$. (B) Electron microscopy image of a collagen pocket (arrow) in a 24 months TTR/HSF1 sciatic nerve. Scale bar: 400 nm.

with TTR deposition was 18645 ± 3048 fibers/mm^2. However, there was a significant decrease in the number of UMF and a small decrease in myelinated fibers in older 24 months TTR/HSF1 mice sciatic nerves with TTR deposition (Fig. 4, chart), which presented an average UMF density of 44570 ± 7229 and MF of 13381 ± 1612 fibers/mm^2, respectively. This decrease was not age-related, as we did not find significative changes in UMF density in 12- and 24-month old control TTR mice (not shown). Furthermore, we observed signs of neurodegeneration in 24 months TTR/HSF1 mice as compared to age matched control TTR mice, namely collagen pockets (Fig. 4, right picture). Collagen pockets are characteristic of FAP nerves and are a consequence of a Schwann cell that lost the axon but continues to produce myelin that involves collagen.

3.5. Hsp70 skin expression

We next investigated the expression of Hsp70 in the skin of transgenic mice with or without TTR deposition. In the wild type background, a rise in Hsp70 expression was observed in skin with non-fibrillar TTR (−/+) or with amyloid (+/+) deposition, as compared to mice without deposition (−/−), which is documented in the pictures of Fig. 5A and in the quantification chart. The same finding was evident when Hsp70 expression in skin was examined by Western blot analysis (Fig. 5B). In contrast, in TTR/HSF1 skin, there was no relationship between TTR deposition and Hsp70 levels, that is, the level of Hsp70 was maintained at background levels despite of TTR deposition, as depicted in Fig. 5A. Therefore, the presence of non-fibrillar and fibrillar aggregates induces a stress response in tissues that do not synthesize TTR, a response regulated by HSF1.

4. Discussion

Protein misfolding diseases result to a certain extent from the incapacity of the cell to stay below the dangerous limits of intra and/or extracellular accumulated aggregated proteins as in Alzheimer's disease, Parkinson's disease or amyotrophic lateral sclerosis. The proteins involved are predisposed to aggregate, forming protofilaments and eventually amyloid fibrils. In the case of FAP, extracellular accumulation of aggregated TTR affects mainly the PNS, leading to inflammatory and oxidative stress and ultimately neurodegeneration. The mechanisms by which the various TTR mutations lead to amyloid aggregation have been the focus of research for two decades. Development of therapeutic strategies in FAP entails, among others, not only the elucidation of molecular mechanism leading to fibril formation but also the cellular/tissue effects produced by TTR deposition. Whilst the former aspect has gained some insights due to intense research at the *in vitro* level, the latter issue has not been properly addressed, in part due to the lack of appropriate animal models with TTR deposition in the PNS. Recently, a *Drosophila* model expressing variant TTR was established

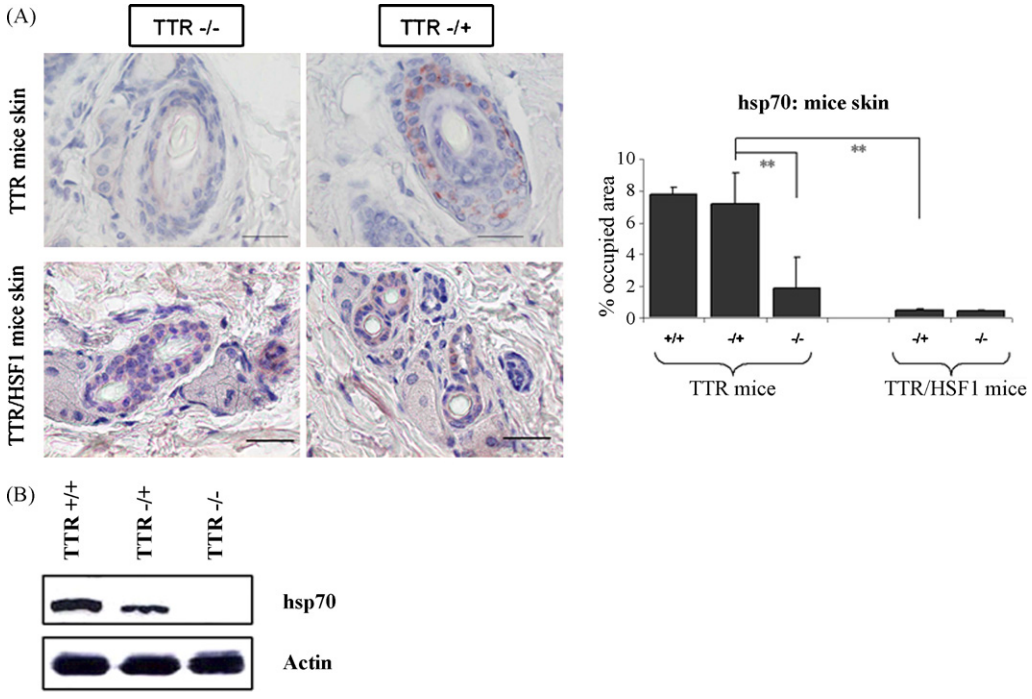

Fig. 5. TTR deposition and Hsp70 expression in mice skin. (A) Top pictures represent skin from the TTR mice strain, without (−/−; $n = 7$) and with (−/+; $n = 7$) TTR deposition and with amyloid deposition (+/+; $n = 2$); bottom pictures represent skin from the TTR/HSF1 mice strain, without (−/−; $n = 4$) and with (−/+; $n = 6$) TTR deposition. Scale bar 30 μm. The chart represents a semi-quantitative analysis of the Hsp70 immunohistochemical data. $^{**}p < 0.002$. (B) Western blot analysis of protein extracts from TTR mice skin probed for Hsp70 and β-actin.

(Pokrzywa et al., 2007). This approach resulted in a model which presented neurodegeneration.

We hypothesized that HSF1 could be involved in FAP pathogenesis as a cell defence mechanism against the presence of TTR extracellular deposits and that disruption of the heat shock response would aggravate TTR deposition. We were successful in the generated mouse model, compared to the previous transgenic for TTR V30M with a full HSF1 response as: (i) deposition in extra-neural tissues was increased, anticipated and recapitulated pathological findings in FAP; (ii) deposition occurred in the PNS; (iii) induction of pro-inflammatory cytokines, RAGE up-regulation, NF-κB activation was evident in the PNS; (iv) deposition did not occur in the brain and spinal cord; (v) a significant decrease in unmyelinated fibers occurred when fibrillar material was evident in nerve.

The increase of extracellular TTR deposition in multiple tissues of TTR/HSF1 mice, including the PNS are suggestive that absence/reduction of HSF1 might result in the impairment for responsiveness of specific Hsps to signals in the external milieu; the intracellular molecular signaling mechanisms involved in such a scenario merit certainly further dissection, as well as the possible intervention of an extracellular chaperone on protein aggregation which cannot be ruled out at this point.

Many studies have pointed towards an important role of HSF1 and Hsps during neurodegeneration as protective effectors. HSF1 can protect by regulating Hsps expression and Hsps by interacting with aberrantly folded proteins to prevent aggregate formation. In Huntington's disease mice model an active form of HSF1 can prevent the characteristic weight loss and expand survival (Fujimoto et al., 2005). In fly and mouse models of polyglutamine and Parkinson's diseases many reports show the protective influence of Hsps in neurodegeneration. For instance, overexpressing Hsp70 in a *Drosophila* model of Huntington's disease suppresses the aggregation and toxicity of intracellular inclusions (Warrick et al., 1999) and in a Parkinson disease model, the expression of a dominant negative Hsp70 exacerbates the neurodegenerative process (Auluck et al., 2002), while induction of the stress response was used with success to prevent neurodegeneration in amyotrophic lateral sclerosis mouse model (Kieran et al., 2004). In the TTR transgenic model with a full HSF1 response, we observed Hsp70 up-regulation in tissues with TTR deposition, indicating that TTR aggregates are able to induce the stress response, supporting therefore the notion for Hsps protective role that is absent in the TTR/HSF1 mouse model. In this regard, we recently reported up-regulation of a resident endoplasmic reticulum chaperone BiP, belonging to the family of Hsp70, in tissues affected with TTR deposition (Teixeira et al., 2006).

It is known that in aging there is a compromised ability to activate HSF1 and Hsps decrease their activity (Heydari et al., 2000). For instance, Hsp70 induction is compromised in senescent cells (Liu et al., 1991). Probably, that is why protein conformational pathologies appear as age-related diseases. Disease might accelerate the normal progressive decline activity of Hsps and the loss of control in misfolding, and so, increase the organism susceptibility to aggressions. Reports relating HSF1 and aging were studied in *Caenorhabditis elegans* where HSF1 downregulation is able to accelerate aging (Garigan et al., 2002) and later, also in *Caenorhabditis elegans,* a link between polyglutamine aggregation, aging and Hsps was suggested (Hsu et al., 2003) reinforced by the finding that *hsf-1* RNAi accelerated aggregated formation. Other report that supports the link between HSF1 and aggregation concerns Aβ mediated toxicity in *Caenorhabditis elegans* where *hsf-1* RNAi worms have more protein aggregates suggesting that HSF1 protects from proteotoxicity (Cohen et al., 2006).

As for the role of Hsps in intracellular signalling a great deal of research has been performed in cancer, infections, vascular diseases, transplant rejection (for a review see Pockley, 2002) but not yet in FAP research. The stress response has been reported to interfere with inflammatory processes to attenuate its mechanism of injury. Inflammatory stimulus induces expression of TNF-α and IL1-β cytokines which can be prevented by activating HSF1 (Singh et al., 2000; Xie et al., 2002) and by increasing Hsp70 synthesis (Ding et al., 2001) or Hsp27 (Park et al., 1998) which are under the direct control of HSF1. Pro-inflammatory cytokines are known to increase during FAP pathogenesis and possibly trigger a heat shock response by increasing Hsps, as we observed for Hsp70, in the transgenic mouse model with a full heat shock response.

Experimental data is also available on the importance of Hsps on apoptosis: Hsp27 up-regulation has been implicated in sensory and motor neuronal survival after peripheral nerve crush (Benn et al., 2002); besides, Hsp70 was shown to interfere with apoptotic cell program by inhibiting the release of cytochrome *c* from mitochondria and by preventing the processing of procaspases 9 and 3 (Mosser et al., 2000). In FAP, neurodegeneration occurs by caspase-3 activity (Sousa et al., 2001a) and Hsps could act in FAP also at this level.

The TTR/HSF1 model now described allows different studies, not possible until now. Sural nerve biopsies, on which most of the pathological analysis in FAP has been performed, represent a restricted portion of the PNS, and it is clearly possible that TTR deposits in ganglia, or more proximally in nerve trunks, could be responsible for distal nerve fiber loss. The possibility to analyze DRG with deposition in the TTR/HSF1 mouse model is invaluable, and permits a close evaluation of events occurring in sensory and autonomic neurons responsible for neurodegeneration.

Finally, this much awaited model is necessary for evaluation of effective therapeutical drugs and approaches to fight the disease, including targets to the PNS; so far, potential drugs have been tested "in vitro" and encompass small compounds to prevent TTR aggregate formation (Almeida et al., 2004; Cardoso et al., 2007; Johnson et al., 2008; Julius et al., 2007; Reixach et al., 2006). Studies performed in mice to stabilize TTR or to disrupt TTR fibrils were performed (Cardoso and Saraiva, 2006; Tagoe et al., 2007) but could

not evaluate the action in the peripheral nervous system. Presently, these compounds can be tested in these novel transgenic TTR/HSF1 mice and the success in preventing TTR deposition in the peripheral nervous system evaluated.

Other avenues for therapy entail action on signaling pathways involving RAGE or other mediators; with the present work, manipulation of the stress response can be viewed as a novel potential pharmacological approach in FAP.

Acknowledgements

We are grateful to Tânia Ribeiro for mice maintenance, Fátima Ferreirinha and Maria José Ferreira for morphometric analysis, Rossana Correia for tissue processing, António Guimarães from Hospital de Santo António, Porto, for interpretation of pathological findings and Max Gottesman from Columbia University for helpful discussion. We are indebted to Dr. Shuishiro Maeda from Yamanashi University for providing the human V30M transgenics and Ivor Benjamin for Hsf1-KO mice.

The work was supported by grants from Fundação para a Ciência e Tecnologia from Portugal, through a post-doctoral fellowship (SFRH/BPD/20738/2004) and POCTI and POCI programs.

Disclosure statement: There is no conflict of interest to disclose.

References

Almeida, M.R., Macedo, B., Cardoso, I., Alves, I., Valencia, G., Arsequell, G.A., Saraiva, M.J., 2004. Selective binding to transthyretin and tetramer stabilization in serum from patients with familial amyloidotic polyneuropathy by an iodinated diflunisal derivative. Biochem. J. 381, 351–356.

Auluck, P.K., Chan, H.Y., Trojanowski, J.Q., Lee, V.M., Bonini, N.M., 2002. Chaperone suppression of alpha-synuclein toxicity in a *Drosophila* model for Parkinson's disease. Science 295, 865–868.

Benn, S.C., Perrelet, D., Kato, A.C., Scholz, J., Decosterd, I., Mannion, R.J., Bakowska, J.C., Woolf, C.J., 2002. Hsp27 upregulation and phosphorylation is required for injured sensory and motor neuron survival. Neuron 36, 45–56.

Cardoso, I., Saraiva, M.J., 2006. Doxycycline disrupts transthyretin amyloid: evidence from studies in a FAP transgenic mice model. FASEB J. 20, 234–239.

Cardoso, I., Almeida, M.R., Ferreira, N., Arsequell, G., Valencia, G., Saraiva, M.J., 2007. Comparative in vitro and ex vivo activities of selected inhibitors of transthyretin aggregation: relevance in drug design. Biochem. J. 408, 131–138.

Cohen, E., Bieschke, J., Perciavalle, R.M., Kelly, J.W., Dillin, A., 2006. Opposing activities protect against age-onset proteotoxicity. Science 313, 1604–1610.

Coimbra, A., Andrade, C., 1971. Familial amyloid polyneuropathy: an electron microscope study of the peripheral nerve in five cases. I. Interstitial changes. Brain 94, 199–206.

Ding, X.Z., Fernandez-Prada, C.M., Bhattacharjee, A.K., Hoover, D.L., 2001. Over-expression of hsp-70 inhibits bacterial lipopolysaccharide-induced production of cytokines in human monocyte-derived macrophages. Cytokine 16, 210–219.

Fujimoto, M., Takaki, E., Hayashi, T., Kitaura, Y., Tanaka, Y., Inouye, S., Nakai, A., 2005. Active HSF1 significantly suppresses polyglutamine aggregate formation in cellular and mouse models. J. Biol. Chem. 280, 34908–34916.

Garigan, D., Hsu, A.L., Fraser, A.G., Kamath, R.S., Ahringer, J., Kenyon, C., 2002. Genetic analysis of tissue aging in *Caenorhabditis elegans*: a role for heat-shock factor and bacterial proliferation. Genetics 161, 1101–1112.

Heydari, A.R., You, S., Takahashi, R., Gutsmann-Conrad, A., Sarge, K.D., Richardson, A., 2000. Age-related alterations in the activation of heat shock transcription factor 1 in rat hepatocytes. Exp. Cell. Res. 256, 83–93.

Hsu, A.L., Murphy, C.T., Kenyon, C., 2003. Regulation of aging and age-related disease by DAF-16 and heat-shock factor. Science 300, 1142–1145.

Johnson, S.M., Connelly, S., Wilson, I.A., Kelly, J.W., 2008. Biochemical and structural evaluation of highly selective 2-arylbenzoxazole-based transthyretin amyloidogenesis inhibitors. J. Med. Chem. 51, 260–270.

Julius, R.L., Farha, O.K., Chiang, J., Perry, L.J., Hawthorne, M.F., 2007. Synthesis and evaluation of transthyretin amyloidosis inhibitors containing carborane pharmacophores. Proc. Natl. Acad. Sci. USA 104, 4808–4813.

Kaplan, B., German, G., Ravid, M., Pras, M., 1994. Determination of amyloid type by ELISA using milligram amounts of tissue. Clin. Chim. Acta 229, 171–179.

Kieran, D., Kalmar, B., Dick, J.R., Riddoch-Contreras, J., Burnstock, G., Greensmith, L., 2004. Treatment with arimoclomol, a coinducer of heat shock proteins, delays disease progression in ALS mice. Nat. Med. 10, 402–405.

Liu, A.Y., Choi, H.S., Lee, Y.K., Chen, K.Y., 1991. Molecular events involved in transcriptional activation of heat shock genes become progressively refractory to heat stimulation during aging of human diploid fibroblasts. J. Cell. Physiol. 149, 560–566.

Mosser, D.D., Caron, A.W., Bourget, L., Meriin, A.B., Sherman, M.Y., Morimoto, R.I., Massie, B., 2000. The chaperone function of hsp70 is required for protection against stress-induced apoptosis. Mol. Cell. Biol. 20, 7146–7159.

Nagata, Y., Tashiro, F., Yi, S., Murakami, T., Maeda, S., Takahashi, K., Shimada, K., Okamura, H., Yamamura, K., 1995. A 6-kb upstream region of the human transthyretin gene can direct developmental, tissue-specific, and quantitatively normal expression in transgenic mouse. J. Biochem. (Tokyo) 117, 169–175.

Park, Y.M., Han, M.Y., Blackburn, R.V., Lee, Y.J., 1998. Overexpression of HSP25 reduces the level of TNF alpha-induced oxidative DNA damage biomarker, 8-hydroxy-2′-deoxyguanosine, in L929 cells. J. Cell. Physiol. 174, 27–34.

Pockley, A.G., 2002. Heat shock proteins, inflammation, and cardiovascular disease. Circulation 105, 1012–1017.

Pokrzywa, M., Dacklin, I., Hultmark, D., Lundgren, E., 2007. Misfolded transthyretin causes behavioral changes in a *Drosophila* model for transthyretin-associated amyloidosis. Eur. J. Neurosci. 26, 913–924.

Puchtler, H., Sweat, F., 1965. Congo red as a stain for fluorescence microscopy of amyloid. J. Histochem. Cytochem. 13, 693–694.

Reixach, N., Adamski-Werner, S.L., Kelly, J.W., Koziol, J., Buxbaum, J.N., 2006. Cell based screening of inhibitors of transthyretin aggregation. Biochem. Biophys. Res. Commun. 348, 889–897.

Santos, S.D., Saraiva, M.J., 2004. Enlarged ventricles, astrogliosis and neurodegeneration in heat shock factor 1 null mouse brain. Neuroscience 126, 657–663.

Saraiva, M.J., Birken, S., Costa, P.P., Goodman, D.S., 1984. Amyloid fibril protein in familial amyloidotic polyneuropathy, Portuguese type. Definition of molecular abnormality in transthyretin (prealbumin). J. Clin. Invest. 74, 104–119.

Sasaki, H., Tone, S., Nakazato, M., Yoshioka, K., Matsuo, H., Kato, Y., Sakaki, Y., 1986. Generation of transgenic mice producing a human transthyretin variant: a possible mouse model for familial amyloidotic polyneuropathy. Biochem. Biophys. Res. Commun. 139, 794–799.

Singh, I.S., Viscardi, R.M., Kalvakolanu, I., Calderwood, S., Hasday, J.D., 2000. Inhibition of tumor necrosis factor-alpha transcription in macrophages exposed to febrile range temperature. A possible role for

heat shock factor-1 as a negative transcriptional regulator. J. Biol. Chem. 275, 9841–9848.

Sousa, M.M., Saraiva, M.J., 2003. Neurodegeneration in familial amyloid polyneuropathy: from pathology to molecular signaling. Prog. Neurobiol. 71, 385–400.

Sousa, M.M., Yan, S.D., Stern, D., Saraiva, M.J., 2000. Interaction of the receptor for advanced glycation end products (RAGE) with transthyretin triggers nuclear transcription factor kB (NF-κB) activation. Lab. Invest. 80, 1101–1110.

Sousa, M.M., Cardos, o I., Fernandes, R., Guimaraes, A., Saraiva, M.J., 2001a. Deposition of transthyretin in early stages of familial amyloidotic polyneuropathy: evidence for toxicity of nonfibrillar aggregates. Am. J. Pathol. 159, 1993–2000.

Sousa, M.M., Du Yan, S., Fernandes, R., Guimaraes, A., Stern, D., Saraiva, M.J., 2001b. Familial amyloid polyneuropathy: receptor for advanced glycation end products-dependent triggering of neuronal inflammatory and apoptotic pathways. J. Neurosci. 21, 7576–7586.

Sousa, M.M., Fernandes, R., Palha, J.A., Taboada, A., Vieira, P., Saraiva, M.J., 2002. Evidence for early cytotoxic aggregates in transgenic mice for human transthyretin Leu55Pro. Am. J. Pathol. 161, 1935–1948.

Sousa, M.M., do Amaral, J.B., Guimaraes, A., Saraiva, M.J., 2005. Up-regulation of the extracellular matrix remodeling genes, biglycan, neutrophil gelatinase-associated lipocalin, and matrix metalloproteinase-9 in familial amyloid polyneuropathy. FASEB J. 19, 124–126.

Tagoe, C.E., Reixach, N., Friske, L., Mustra, D., French, D., Gallo, G., Buxbaum, J.N., 2007. In vivo stabilization of mutant human transthyretin in transgenic mice. Amyloid 14, 227–236.

Teixeira, P.F., Cerca, F., Santos, S.D., Saraiva, M.J., 2006. Endoplasmic reticulum stress associated with extracellular aggregates: evidence from transthyretin deposition in familial amyloid polyneuropathy. J. Biol. Chem. 281, 21998–22003.

Teng, M.H., Yin, J.Y., Vidal, R., Ghiso, J., Kumar, A., Rabenou, R., Shah, A., Jacobson, D.R., Tagoe, C., Gallo, G., Buxbaum, J., 2001. Amyloid and nonfibrillar deposits in mice transgenic for wild-type human transthyretin: a possible model for senile systemic amyloidosis. Lab. Invest. 81, 385–396.

Warrick, J.M., Chan, H.Y., Gray-Board, G.L., Chai, Y., Paulson, H.L., Bonini, N.M., 1999. Suppression of polyglutamine-mediated neurodegeneration in *Drosophila* by the molecular chaperone HSP70. Nat. Genet. 23, 425–428.

Xiao, X., Zuo, X., Davis, A.A., McMillan, D.R., Curry, B.B., Richardson, J.A., Benjamin, I.J., 1999. HSF1 is required for extra-embryonic development, postnatal growth and protection during inflammatory responses in mice. EMBO J. 18, 5943–5952.

Xie, Y., Chen, C., Stevenson, M.A., Auron, P.E., Calderwood, S.K., 2002. Heat shock factor 1 represses transcription of the IL-1beta gene through physical interaction with the nuclear factor of interleukin 6. J. Biol. Chem. 277, 11802–11810.

Yamamura, K., Wakasugi, S., Maeda, S., Inomoto, T., Iwanaga, T., Uehira, M., Araki, K., Miyazaki, J., Shimada, K., 1987. Tissue-specific and developmental expression of human transthyretin gene in transgenic mice. Dev. Genet. 8, 195–205.